Prevention of Burn Wound Progression by Mesenchymal Stem Cell Transplantation

Deeper Insights Into Underlying Mechanisms

Ozan Luay Abbas, MD, Orhan Özatik, MD,† Zeynep Burçin Gönen, DDs, PhD,‡ Serdal Öğüt, PhD,§ Emre Entok, MD,|| Fikriye Yasemin Özatik, MD,¶ Dilek Bahar, MSc,‡ Zehra Burcu Bakır, PhD,# and Ahmet Musmul, PhD***

Introduction: Burns are dynamic wounds that may present a progressive expansion of necrosis into the initially viable zone of stasis. Therefore, salvage of this zone is a major subject of focus in burn research. The beneficial effects of mesenchymal stem cells (MSCs) on the survival of the zone of stasis have been previously documented. However, many gaps still exist in our knowledge regarding the underlying protective mechanisms. Hence, this study was designed to evaluate the pathophysiological basis of MSCs in the prevention of burn wound progression.

Methods: Wistar rats received thermal trauma on the back according to the "comb burn" model. Animals were randomly divided into sham, control, and stem cell groups with sacrifice and analysis at 72 hours after the burn. The stasis zones were evaluated using histochemistry, immunohistochemistry, biochemistry, real-time polymerase chain reaction assay, and scintigraphy to evaluate the underlying mechanisms.

Results: Gross evaluation of burn wounds revealed that vital tissue percentage of the zone of stasis was significantly higher in the stem cell group. Semiquantitative grading of the histopathologic findings showed that MSCs alleviated burn-induced histomorphological alterations in the zone of stasis. According to CC3a staining and expression analysis of Bax (B-cell leukemia 2–associated X) and Bcl-2 (B-cell leukemia 2) genes, MSCs attenuated increases in apoptosis postburn. In addition, these transplants showed an immunomodulatory effect that involves reduced neutrophilic infiltration, down-regulation of proinflammatory cytokines (tumor necrosis factor α, interleukin 1β [IL-1β], and IL-6), and up-regulation of the anti-inflammatory cytokine IL-10 in the zone of stasis. Burn-induced oxidative stress was significantly relieved with MSCs, as shown by increased levels of malondialdehyde, whereas the expression and activity of the antioxidant enzyme superoxide dismutase were increased. Finally, MSC-treated interspaces had enhanced vascular density with higher expression levels for vascular endothelial growth factor A, platelet-derived growth factor, fibroblast growth factor, and transforming growth factor β. Gamma camera images documented better tissue perfusion in animals treated with MSCs.

Conclusions: The protective effects of MSCs are mediated by the inhibition of apoptosis through immunomodulatory, antioxidative, and angiogenic actions.

Key Words: angiogenesis, apoptosis, burn, mesenchymal stem cell, oxidative stress, stasis zone

(*Ann Plast Surg* 2018;81: 715–724)

Burns are dynamic wounds that may present a progressive expansion of necrosis into viable neighboring tissues. The initial pattern of thermal injury is characterized by a central zone of irreversible tissue damage surrounded by a potentially salvageable stasis zone.[1] In face of suboptimal treatment, the initially viable tissue in the stasis zone may progress to coagulation necrosis through several mechanisms during the first few days following the burn.[2] This progression is clinically relevant because it influences the extent and depth of a burn, which are the key determinants of morbidity and mortality.[3]

Although both apoptosis and necrosis have been shown to contribute to cell death during burn wound progression, several studies suggested a prominent role of apoptosis.[4,5] While necrotic cell death is thought to be an unpreventable passive event that results from the direct effects of the thermal trauma, apoptosis can be thought of as resulting from preventable secondary damage from the burn.[6] The pathophysiology of burn-induced apoptosis involves highly complicated mechanisms, and recent studies have shown that prolonged inflammatory reaction, oxidative stress, and impaired tissue perfusion are central to this event.[7] Therefore, a logical strategy to save the stasis zone would be to limit apoptosis by ameliorating these secondary sources of tissue damage. From this point of view, mesenchymal stem cells (MSCs) are an attractive choice because of their ability to differentiate, modulate immune response, and provide trophic support.[8]

The beneficial effects of MSCs on wound healing were documented in many in vivo models and in reported clinical cases.[9–22] In these studies, MSCs were applied either directly into the burn site (zone of coagulation) or systemically. All evaluations were made in tissues obtained from the burn area (zone of coagulation). Despite this large number of studies, only 2 studies evaluated the effects of MSCs on burn wound progression and found that the implantation of these cells exerts benefits for the survival of the stasis zone.[23,24] However, many gaps still exist in our knowledge regarding the protective mechanisms of MSCs in the prevention of burn wound progression and local tissue effects. Hence, we designed this study to evaluate the pathophysiological basis of MSCs in the prevention of burn wound progression. Considering that main therapeutic effects of such cells are mediated by paracrine mechanisms,[25] we focused on how these cells could limit burn wound progression rather than their transdifferentiation.

Received February 20, 2018, and accepted for publication, after revision July 12, 2018.

From the Departments of *Plastic, Reconstructive and Aesthetic Surgery and †Histology and Embryology, Faculty of Medicine, Ahi Evran University, Kırşehir; ‡Gen Kök Genome and Stem Cell Center, Erciyes University, Kayseri; §Department of Nutrition and Dietetics, Faculty of Health Science, Adnan Menderes University, Aydın; ||Department of Nuclear Medicine, Faculty of Medicine, Osmangazi University, Eskişehir; ¶Department of Pharmacology, Faculty of Medicine, Ahi Evran University, Kırşehir; #Department of Biology, Adnan Menderes University, Aydın; and **Department of Biostatistics, Faculty of Medicine, Osmangazi University, Eskişehir, Turkey.

Author Contributions: All authors have made substantial contributions to the conception and design of the study, acquisition of data, analysis and interpretation of data, drafting the article and revising it critically for important intellectual content, and final approval of the version to be submitted. O.L.A. is corresponding author; O.Ö.: histological and immunohistological analysis; Z.B.G.: stem cell isolation and characterization; S.Ö.: biochemical evaluation of oxidative stress; E.E.: nuclear imaging; F.Y.Ö.: surgical procedures and data analysis; D.B.: stem cell isolation and characterization; Z.B.B.: collagen assay analysis; A.M.: biostatistical analysis.

This study received approval of Osmangazi University Ethical Committee for Experimental Research on Animals and was supported by Ahi Evran University Research Fund (project TIP.A3.16.012).

Conflicts of interest and sources of funding: none declared.

Reprints: Ozan Luay Abbas, MD, Department of Plastic, Reconstructive and Aesthetic Surgery, Faculty of Medicine, Ahi Evran University, Postal code 40100, Kırşehir, Turkey. E-mail: ozanluay@hotmail.com.

ISSN: 0148-7043/18/8106–0715
DOI: 10.1097/SAP.0000000000001620

METHODS

Ethical Consideration

This study received approval of the Ethical Committee for Experimental Research on Animals. Housing and care of the animals met the criteria outlined by the National Research Council.

Isolation and Culture of Rat Bone Marrow–Derived MSCs

The rat was killed by overdose anesthesia and soaked in 75% alcohol for 1 minute. The bilateral femur and tibia were aseptically excised and washed by phosphate-buffered saline (PBS). After removing the proximal and distal ends of the bones, 21-gauge needle was used to flush the bone marrow cavity with low-glucose Dulbecco modified eagle medium, supplemented with 10% fetal bovine serum and 1% penicillin/streptomycin. Cells were seeded into 25-cm^2 culture flask containing standard culture medium (low-glucose Dulbecco modified eagle medium with 10% fetal bovine serum, 1% penicillin/streptomycin solution, and 1% stable glutamine; Biological Industries, Kibbutz Beit Haemek, Israel) at 37°C and 5% CO_2. After 3 days of first culture, the medium was refreshed and subsequently replaced twice a week. Bone marrow stem cells were isolated on the basis of their adhesiveness to the culture plates. After cells reached 85% to 90% confluent in culture, cells were detached by 0.05% trypsin-EDTA solution for 4 minutes. The cells were washed with PBS (Biological Industries) and replated at 1:4 ratio for subculture. Mesenchymal stem cells from passage 3 were used.

Labeling of MSCs

Mesenchymal stem cells were transfected by the Neon transfection system (Invitrogen) at room temperature using one 1200-voltage, 20-millisecond pulse to express green fluorescence protein (GFP) before transplantation. Mesenchymal stem cell viability was measured by trypan blue (Sigma T8154) under an invert microscope at the day of transfection and 24 hours later.

Characterization of MSCs by Flow Cytometry

Immunophenotyping characterization of MSCs was performed with antibodies against the CD11b, CD29, CD44, CD45, CD73, CD90, and CD105 antigens. All antibodies were from BD Biosciences. Flow cytometry was performed by using Navios (Beckman Coulter, USA). The data were analyzed with Kaluza software (Beckman Coulter, USA). More than 50% staining was regarded as positive.

Count and Viability Assay

Viable cells were detected by using dual fluorescent probes of Muse Count & Viability Assay Kit (Merck Millipore, Germany) on a flow cytometer (Muse EasyCyte; Merck Millipore).

Burn Injury Model

Burn wounds were created according to a previously described contact thermal trauma model.[26] In this model, a brass comb with 4 prongs separated by 3 notches is used to produce 4 burn sites (coagulation zones) separated by 3 unburned interspaces (stasis zones). The comb was preheated in boiling water for 5 minutes and then placed on the shaved dorsal skin of each anesthetized animal and held for 30 seconds with gravity alone. No postburn dressing was applied.

Experimental Design

Fifty adult male Wistar rats (300–325 g) were randomly divided into 3 groups as follows:

(1) Stem cell group (n = 20): Thirty minutes after burn induction, 0.2 mL of PBS containing 1×10^6 MSCs was uniformly injected subcutaneously to each interspace.
(2) Control group (n = 20): Thirty minutes after burn induction, 0.2 mL of PBS was injected into the subcutaneous plane of each interspace.
(3) Sham group (n = 10): The comb was placed in 25°C water and applied on the back of each rat. Thereafter, 0.2 mL of PBS was given subcutaneously to the corresponding areas of unburned skin.

Seventy-two hours after the burn, 10 rats were randomly selected from the control and stem cell groups for scintigraphic evaluation. In the remaining animals, gross examination of burn wounds was performed. Thereafter, the exact areas of the 3 interspaces were biopsied. One band of the interspace with 2 mm of burned skin on each side was used for histological and immunohistochemical evaluations, whereas the remaining 2 bands of interspace skin (without burn tissue) were used for biochemical and genetic evaluations.

Gross Assessment of the Burn Wound

Seventy-two hours after the burn, the animals were reanesthetized, and the viable interspace areas were determined. To this end, a template was drawn on each interspace, and the viable area was outlined. The template was then scanned on a computer, and the survival area was measured as a percentage of the total interspace using Adobe Photoshop CS5 (Adobe Systems, Inc, San Jose, Calif).

Scintigraphic Assessment

Scintigraphic evaluation was performed in 10 randomly selected rats from the control and stem cell groups.[27] Animals were injected with 3 mCi of technetium Tc 99m methoxyisobutylisonitrile through the femoral vein. After 30 minutes, the dorsal wounded areas were excised with 1-cm margins. The specimens were immediately put under a gamma camera, and images were obtained with a pinhole collimator for 15 minutes with a 256 × 256 matrix.

Histological Analysis

Histological examination was performed on hematoxylin-eosin (H&E)–stained sections using conventional microscopy. A systematic examination of 20 random fields under 40× magnification was performed in order to semiquantitatively score the following histological variables (0, none; 1, mild; 2, moderate; 3, severe)[28]: epidermal desquamation, collagen disorganization, fluid shift, leukocyte infiltration, and damage to the skin appendages.

Immunohistochemical Analysis

Skin biopsies were probed with anti–cleaved caspase 3a antibodies (CC3a; Thermo Scientific, Waltham, Mass) for evidence of apoptosis,[29] anti–high mobility group box 1 antibodies (HMGB1; Thermo Scientific) for evidence of necrosis,[29] antimalondialdehyde antibodies (Thermo Scientific) for evidence of oxidative stress, and anti-CD31 antibodies (Thermo Scientific) to identify endothelial cells. All staining procedures were performed according to the manufacturers' instructions. For each antibody, the number of stained cells was determined at 40× magnification, and the mean value of 20 random fields per slide for each animal was used.

Measurement of Tissue Malondialdehyde Level

Tissue malondialdehyde, as a marker of oxidative stress, was determined in tissue homogenates of the skin by thiobarbituric acid reaction. The principle of this technique is based on measuring absorbance of the pink color produced by the interaction of thiobarbituric acid with malondialdehyde at 532 nm.[30]

Measurement of Superoxide Dismutase Activity

Superoxide dismutase (SOD) enzyme activity was measured in tissue homogenates of the skin based on a previously described method.[31]

This method is based on the principle that SOD neutralizes superoxide anion radical produced by xanthine/xanthine oxidase system and subsequently blocks the reduction of water-soluble tetrazolium salt to water-soluble tetrazolium salt formazan.

Measurement of Myeloperoxidase Activity

Activity of myeloperoxidase was determined in tissue homogenates according to a previously described method.[32] Following a series of reactions with hexadecyltrimethylammonium bromide, H_2O_2 solution, and *o*-dianisidine, 1 unit of enzyme activity was defined as the amount of myeloperoxidase that changes the absorbance measured at 460 nm for 3 minutes.

Real-Time Polymerase Chain Reaction Analysis

Real-time polymerase chain reaction (RT-PCR) assay was performed in order to determine the mRNA expression levels of selected inflammatory cytokines (tumor necrosis factor α [TNF-α], interleukin 1β [IL-1β], IL-6, and IL-10), angiogenic growth factors (vascular endothelial growth factor A [VEGF-A], platelet-derived growth factor [PDGF], basic fibroblast growth factor [FGF], and transforming growth factor β [TGF-β]), antioxidant SOD, and apoptotic proteins (B-cell leukemia 2 [Bcl-2] and B-cell leukemia 2–associated X [Bax]) using Light Cycler Fast Start DNA Master SYBR Green I Kit (Roche Diagnostics GmbH, Mannheim, Germany). Housekeeping gene β-actin served as internal control. Primer sequences of the target genes are shown in Table 1.

TABLE 1. Primers Used for RT-PCR Analysis

Gene	Sequence
TNF-α	
Forward	CAGCAACTCCAGAACACCCT
Reverse	GGAGGGAGATGTGTTGCCTC
IL-1β	
Forward	CACCTCTCAAGCAGAGCACAG
Reverse	GGGTTCCATGGTGAAGTCAAC
IL-6	
Forward	TCCTACCCCAACTTCCAATGCTC
Reverse	TTGGATGGTCTTGGTCCTTAGCC
IL-10	
Forward	TTGAACCACCCGGCATCTAC
Reverse	TGGAGAGAGGTACAAACGAGGT
VEGF-A	
Forward	GTCACCGTCGACAGAACAGT
Reverse	GACCCAAAGTGCTCCTCGAA
PDGF	
Forward	TTCTTGATCTGGCCCCCAT
Reverse	TTGACGCTGCTGGTGTTACAG
Basic FGF	
Forward	AGCGGCTCTACTGCAAGAAC
Reverse	GCCGTCCATCTTCCTTCATA
TGF-β	
Forward	AAGAAGTCACCCGCGTGCTA
Reverse	TGTGTGATGTCTTTGGTTTTGTC
SOD	
Forward	GAGCATTCCATCATTGGCCG
Reverse	GGCAATCCCAATCACACCAC
Bcl-2	
Forward	GGATGACTTCTCTCGTCGCT
Reverse	GACATCTCCCTGTTGACGCT
Bax	
Forward	CAAGAAGCTGAGCGAGTGTCT
Reverse	CCCCAGTTGAAGTTGCCGT
β-Actin	
Forward	ACAACCTTCTTGCAGCTCCTC
Reverse	CTGACCCATACCCACCATCAC

Collagen Assay Method

Hydroxyproline was chosen to determine the collagen content of the tissues. Hydroxyproline was determined as previously described.[33] For the assay, the tissue was stored in phosphate buffer until homogenization. Homogenization was performed with a homogenizator for 1 minute. Aliquots of hydroxyproline standards (20–90 μg/mL) and the homogenates were mixed gently with 2 N NaOH in a total volume of 100 μL. The samples were hydrolyzed by autoclaving at 120°C for 20 minutes. Then 900 μL of chloramine-T was added to the samples, and the oxidation was allowed to proceed for 25 minutes at room temperature. Finally, a chromophore was developed by adding 1000 μL Ehrlich reagent and incubating the samples at 65°C for 20 minutes. The absorbance of reddish purple complex was measured at 550 nm using a Shimadzu UV-1601 spectrophotometer (Kyoto, Japan). Absorbance values were plotted against the concentration of standard hydroxyproline, and the presence of hydroxyproline in unknown tissue extracts was determined from the standard curve. The collagen content of the tissues was calculated from assuming that 12.5% of collagen is hydroxyproline. Results are expressed as g/100 g of tissue weight.

Statistical Analysis

Data analyses were performed using the Statistical Package for the Social Sciences, version 21.0 (SPSS Inc, Chicago, Ill). Samples with normal distribution were evaluated by independent-samples *t* test and 1-way analysis of variance. Non–normally distributed variables were compared across the groups by using Kruskal-Wallis 1-way analysis of variance on ranks test. Tukey test was used for the multiple comparisons. $P < 0.05$ was considered statistically significant.

RESULTS

MSCs Expressed Commonly Accepted MSC Markers

The flow cytometry analysis data indicated that the cells expressed MSC markers such as CD29 (99.78%), CD44 (90.29%), CD73 (99.31%), CD90 (99.48%), and CD105 (94.76%); and CD45 (1.87%) and CD11b (4%) (Fig. 1). Viability was quantified by flow cytometer analysis after staining with count and viability kit before application, and more than 90% live cells were detected.

Green Fluorescence Protein–Labeled MSCs Were Not Identified in the Unburned Interspaces

Before and after transfection, viability results were figured out in Table 2. Higher number of viable cells of GFP was found at 24 hours than that on the day of transfection. The illumination of the expression of GFP-transfected cells was observed under a fluorescence microscope (Nikon Ti Eclipse) in culture conditions (Fig. 2). However, after 72 hours of transplantation, the labeled cells were not found in any of the sectioned skin specimens.

MSC Transplantation Reduced the Area of Necrosis in the Zone of Stasis

Gross evaluation of burn wounds in animals of the control and stem cell groups revealed more dramatic expansions from the burn sites to the unburned interspaces in the control animals. The mean percentage

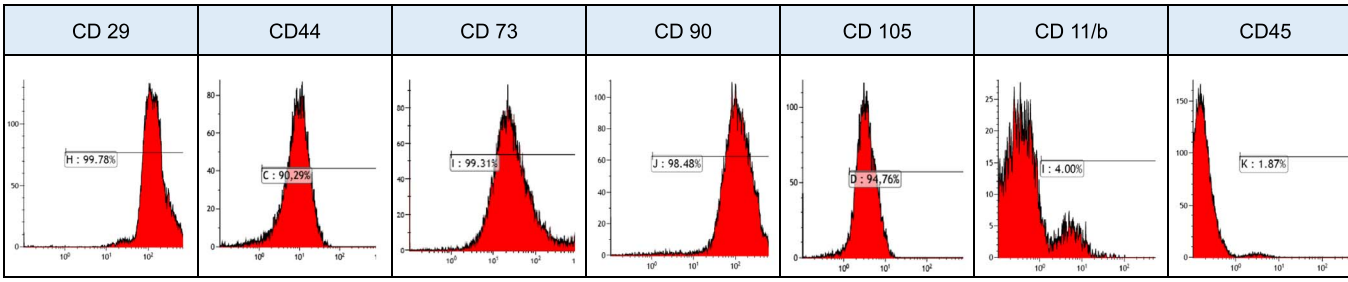

FIGURE 1. Representative flow cytometry analysis of cell-surface markers in MSCs at passage 3. Mesenchymal stem cells expressed MSC markers including CD29, CD 44, CD73, CD90, and CD105, but negative for CD 11b/c and CD45.

of the calculated living area by the paper template method in the stem cell group (33.1% ± 7.58%) was significantly higher than that of the control group (14.8% ± 6.36%) ($P < 0.001$).

MSC Transplantation Alleviated Burn-Induced Histomorphological Alterations in the Zone of Stasis

Histological assessment of H&E-stained sections in the control group documented obvious morphological alterations such as epidermal injury, loose collagen matrix, profound edema, and extensive damage to skin appendages. On the other hand, MSC transplantation markedly attenuated these signs of injury (Fig. 3). Semiquantitative grading of the histopathologic findings revealed significantly higher ($P < 0.001$) damage scores in the control group (Fig. 3). There were no significant differences (all $P > 0.05$) between the sham (0.0241 g/100 g), control (0.0235 g/100 g), and stem cell (0.0232 g/100 g) groups with respect to tissue collagen content.

MSC Transplantation Reduced Apoptotic But Not Necrotic Cell Death in the Zone of Stasis

To evaluate the effects of MSCs on apoptosis, immunohistochemical assessment using antibodies against CC3a was conducted. Compared with the healthy tissues of the sham group, significant increases ($P < 0.001$) in the number of apoptotic cells were observed in the burned tissues of the control and stem cell groups. When both burn groups were compared, the number apoptotic cells in the control group was significantly higher ($P < 0.001$) than that in the stem cell group (Fig. 4).

Bax and Bcl-2 are 2 important regulator genes in the mitochondrial apoptotic pathway. While the product of Bcl-2 gene protects cells from apoptosis, Bax is one of the most important proapoptotic proteins.[34,35] In the control group, the expression of the antiapoptotic Bcl-2 did not show significant changes compared with the sham group ($P = 0.153$). However, significantly up-regulated expression was noticed in the stem cell group ($P < 0.001$). On the other hand, proapoptotic Bax expression in the control group was significantly up-regulated compared with the sham group ($P < 0.001$). This up-regulation was significantly prevented ($P < 0.001$) in the stem cell group, maintaining the level close to the sham values (Fig. 4).

As a marker of cell necrosis, we evaluated the translocation of HMGB1 from the nucleus to the cytoplasm and extracellular space as a signal of cell damage.[29] Healthy tissues of the sham group showed a strict normal nuclear localization of HMGB1, whereas burned tissues of the control and stem cell groups revealed nuclear-to-cytoplasmic and cytoplasmic-to-extracellular redistribution of HMGB1. Compared with the healthy tissues of the sham group, significant increases ($P < 0.01$) in the number of necrotic cells were observed in the burned tissues of the control and stem cell groups. However, there was no significant difference ($P = 0.087$) between both burn groups with respect to necrotic cell count (Fig. 5).

TABLE 2. Rates of Viable MSCs Before and After Transfection

	Rate of Viable MSCs	
Before transfection	95.3%	
After transfection	Day of transfection	66.71%
	24 h after transfection	87.48%

MSC Transplantation Alleviated Early Inflammatory Response to Thermal Trauma

Examination of H&E-stained sections revealed that the number of infiltrating neutrophils significantly increased ($P < 0.001$) after the burn, and MSC transplantation significantly decreased ($P < 0.001$) this elevation. Correspondingly, myeloperoxidase activity, indicative of tissue neutrophil accumulation, was increased significantly ($P < 0.001$) after the burn, and MSC transplantation prevented this alteration ($P < 0.001$) (Fig. 6).

We then evaluated the expression of selected inflammatory cytokines using RT-PCR. Compared with the baseline levels of the sham group, the relative expression levels of the proinflammatory cytokines TNF-α, IL-6, and IL-1β significantly increased ($P < 0.001$) in the control group. In addition, the expression of the anti-inflammatory cytokine IL-10 significantly ($P < 0.01$) elevated. After MSC transplantation, the relative expression levels of the aforementioned proinflammatory cytokines displayed significant reductions ($P < 0.001$) in comparison with

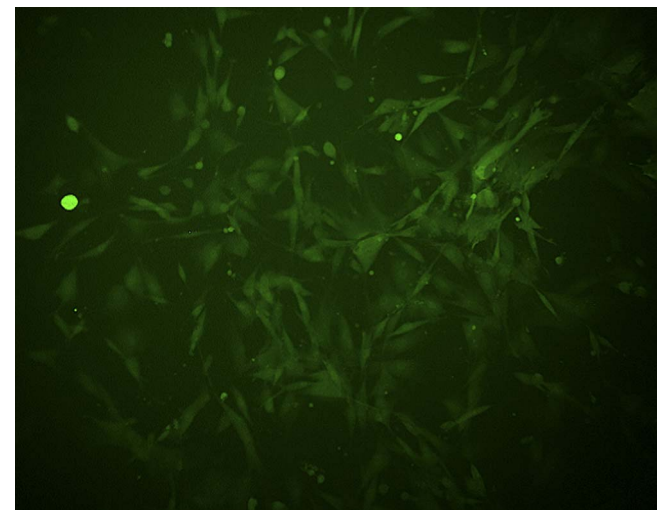

FIGURE 2. The illumination of the GFP-transfected cells was observed under a fluorescence microscope in culture conditions.

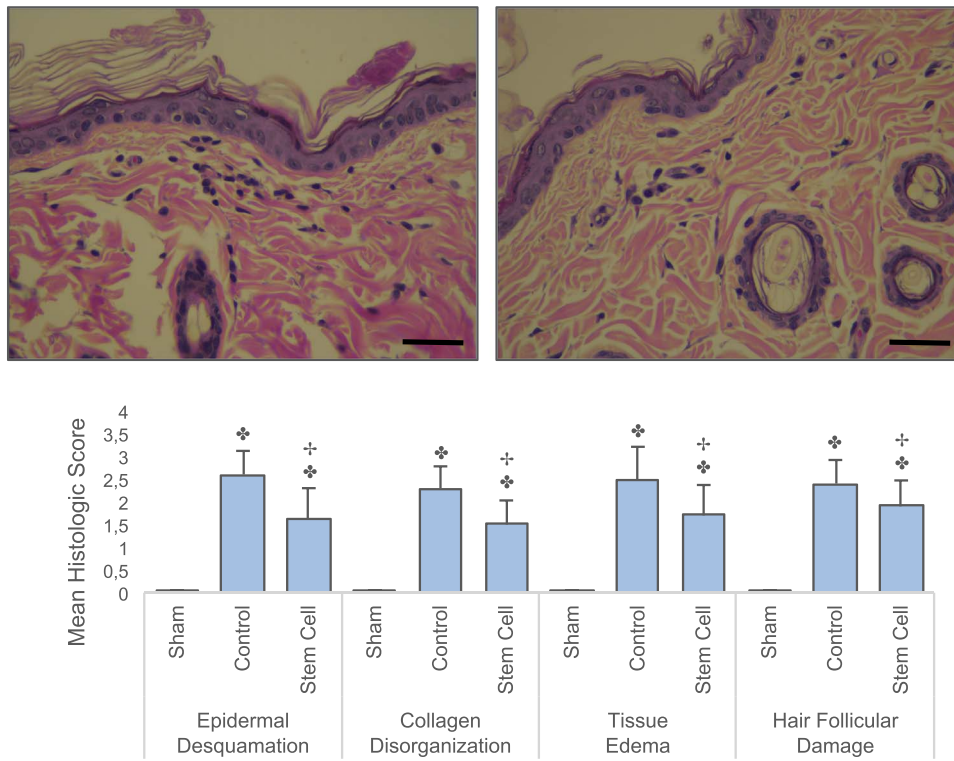

FIGURE 3. Hematoxylin-eosin staining of burn wounds in the control and stem cell groups 72 hours after burn (above). Note the following histological characteristics in the control group: marked epidermal injury, loose collagen matrix with profound interstitial edema, and extensive damage in the hair follicles (above, left). On the other hand, MSC transplantation markedly attenuated these signs of injury (above, right) (×40 magnification). Scales = 100 μm. Semiquantitative assessment of burn-related morphological alterations in hematoxylin-eosin–stained sections (below). The sample size was n = 10 for each group. Data are presented as mean ± SD. ✣$P < 0.001$ versus sham; ✢$P < 0.001$ versus control.

the control group. Furthermore, the elevation of the anti-inflammatory cytokine IL-10 became more significant ($P < 0.001$) (Fig. 6).

MSC Transplantation Relieved Burn-Induced Oxidative Stress in the Zone of Stasis

Tissue malondialdehyde level, as a marker of oxidative stress, was evaluated by thiobarbituric acid reaction. Compared with the healthy tissues of the sham group, burned tissues obtained from control rats presented with elevated malondialdehyde levels ($P < 0.001$). On the other hand, MSC transplantation significantly decreased ($P < 0.001$) this elevation. Correspondingly, immunohistochemical labeling of malondialdehyde revealed higher number of stained cells in the control group in comparison with the stem cell group (Fig. 7).

We then evaluated the local expression of antioxidant SOD using RT-PCR. In comparison with baseline levels of the sham group, significantly decreased ($P < 0.001$) expression levels were detected in the control group. However, MSC transplantation significantly decreased ($P < 0.001$) this reduction. Correspondingly, we documented a significant reduction ($P < 0.001$) in the activity of SOD after the burn, and MSC transplantation significantly ($P < 0.001$) decreased this down-regulation (Fig. 7).

MSC Transplantation Increased Capillary Density and Enhanced Tissue Perfusion in the Zone of Stasis Through the Expression of Various Proangiogenic Factors

To investigate the effects MSCs on neovascularization, the capillaries that were counted on H&E-stained slices were confirmed by CD31 immunostaining. The number of CD31-positive vessels in the stem cell group was significantly ($P < 0.001$) higher than either the control or sham group (Fig. 8).

Scintigraphic evaluation gave information about the circulation status of burn wounds. Visual examination of static images revealed that the uptake of the radioactive marker by burn sites was too low in both burn groups. However, it was difficult to map out the borders of the burn areas in images of the control group. On the other hand, there were obvious borders between the viable and necrotic areas in the images of the stem cell group (Fig. 8). Moreover, quantitative assessment documented that the average radioactivity uptake in the stem cell group was significantly ($P < 0.001$) higher than that in the control group (Fig. 8).

We finally evaluated the expression of some candidate factors that could mediate the obtained vasculotropic effects. Compared with the baseline levels of the sham group, the relative expression levels of the proangiogenic factors VEGF-A, PDGF, basic FGF, and TGF-β significantly increased ($P < 0.001$) in control animals. After MSC transplantation, the up-regulation of expressions became more significant ($P < 0.001$) (Fig. 8).

DISCUSSION

In this study, we investigated the effects of MSCs on burn wound progression and found that MSC transplantation significantly reduced the area of necrosis in the zone of stasis. This finding is in line with results from Öksüz et al[23] and Singer et al,[24] who both reported similar beneficial results in similar models after MSC application. Although the results of such animal studies cannot always be extrapolated directly to humans,[36] we think that they are predictive of human

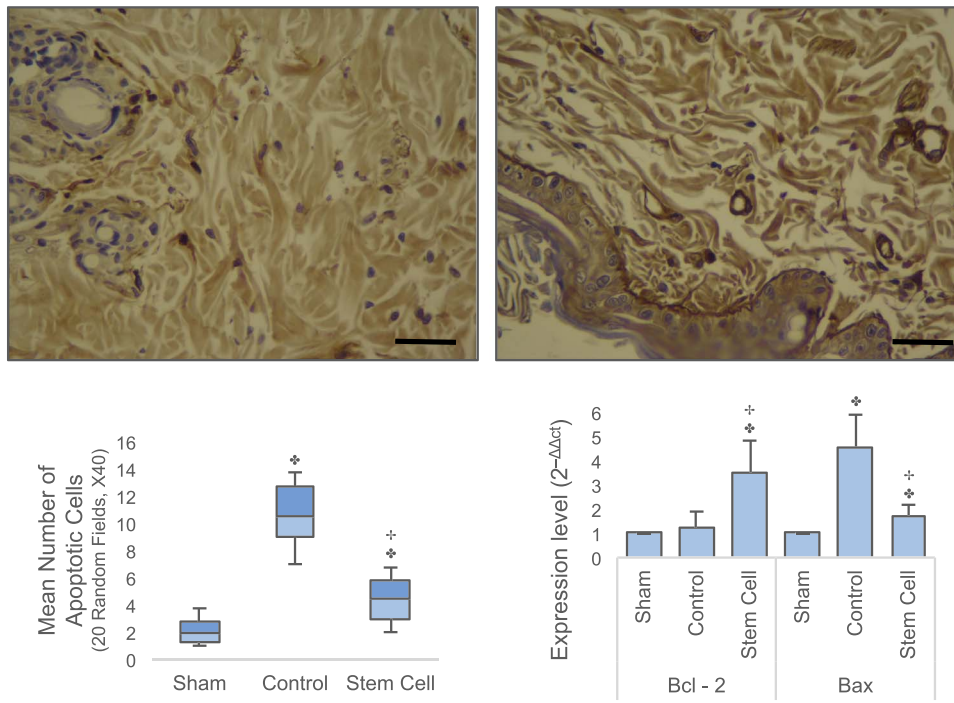

FIGURE 4. Evaluation of apoptosis in the zone of stasis using immunohistochemical labeling of caspase-3 (above). Higher numbers of apoptotic cells were observed in the control group (above, left) in comparison with the stem cell group (above, right) (×40 magnification). Scales = 100 μm. Quantitative assessment of apoptotic cell death (below, left) and apoptosis-related gene expression levels (below, right). The sample size was n = 10 for each group. Data are presented as mean ± SD. ✣$P < 0.001$ versus sham; ✢$P < 0.001$ versus control.

responses and suggestive of the protective potential of MSCs against burn wound progression.

Further histological assessment revealed that MSC application effectively ameliorated the histopathologic changes associated with burn wound progression. The main observed histopathologic improvements were significant decreases in tissue edema, contributing to better tissue perfusion; less damage to adnexal structures that act as a reservoir of keratinocytes and stem cells, resulting in better epidermal proliferation; and longer microscopic length of survived epidermis, indicating limited expansion of burn injury.

Despite the aforementioned beneficial results after MSC transplantation, GFP-labeled cells could not be detected in any of the sectioned skin specimens. This is because evaluations occurred at a time point at which it is highly unlikely that MSCs would integrate into the tissue, differentiate, and replace damaged cells. This finding is in line with the notion that the ability of such cells to modify the tissue microenvironment through trophic support contributes more significantly than their capacity for differentiation in affecting tissue repair.[25] In particular, exosomes have been shown to play a dominant role in paracrine mechanisms.[37–39] Although the exact nature of these paracrine factors

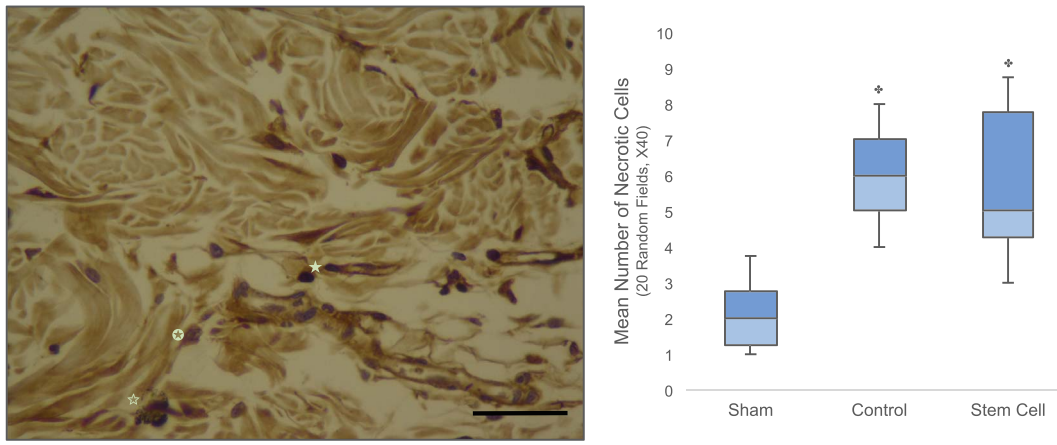

FIGURE 5. Evaluation of necrotic cell death in the zone of stasis using immunohistochemical labeling of HMGB1 (left). HMGB1 was positively stained in the nuclear (★), cytoplasmic (✪), and extracellular (☆) compartments in tissues obtained from the stem cell group (×40 magnification). Scale = 100 μm. Quantitative assessment of necrotic cell death (right). The sample size was n = 10 for each group. Data are presented as mean ± SD. ✣$P < 0.01$ versus sham.

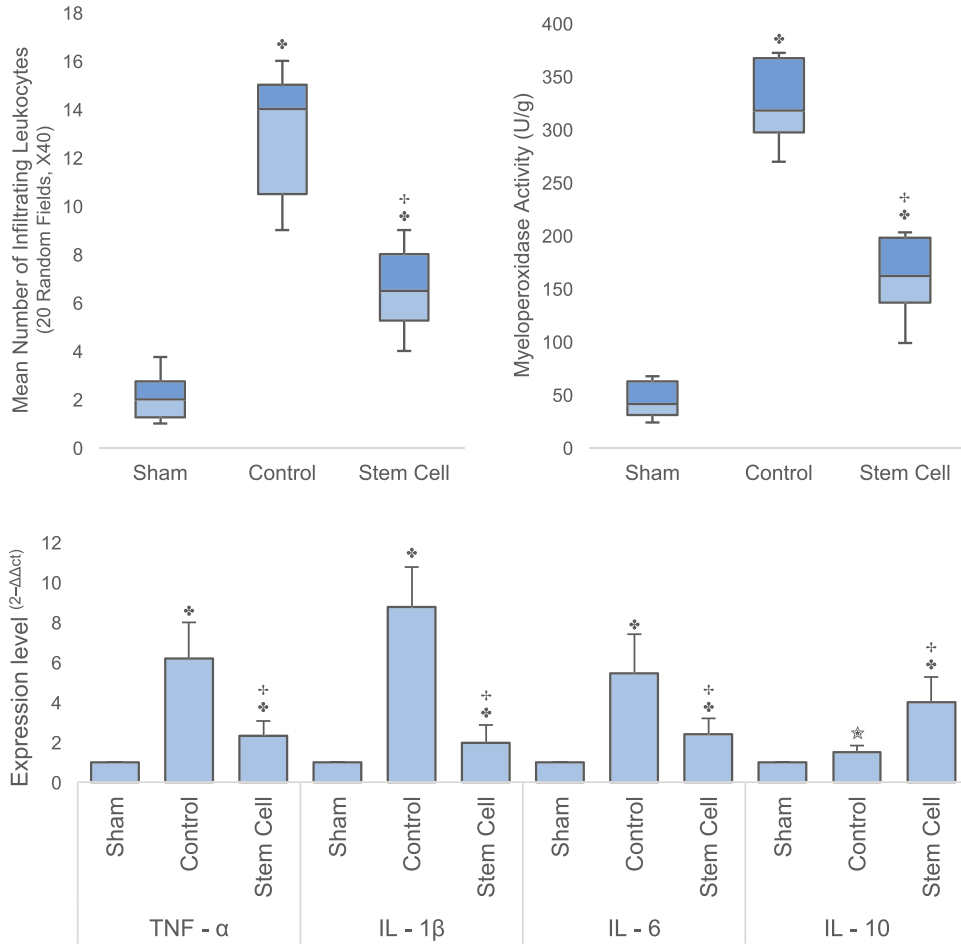

FIGURE 6. Quantitative analyses of infiltrating neutrophils (above left), myeloperoxidase activity (above, right), and inflammatory cytokine expression levels (below). The sample size was n = 10 for each group. Data are presented as mean ± SD. ✣$P < 0.001$ versus sham; ✢$P < 0.001$ versus control; ★$P < 0.01$ versus sham.

remains to be elucidated in further studies, evaluation of local tissue effects around the injected cells gave us information about the local tissue effects and potential mechanisms of action. We documented that the protective effects of MSCs were mediated by the inhibition of apoptosis through immunomodulatory, antioxidative, and angiogenic actions.

Assuming that apoptosis in the zone of stasis is causally linked to the progression of burn wounds,[7] we examined apoptotic cell death immunohistochemically and observed that MSC transplantation substantially ameliorated burn-induced apoptosis in the zone of stasis. Moreover, genetic evaluation revealed that MSCs prevented the up-regulation of proapoptotic Bax, while further up-regulating the expression of antiapoptotic Bcl2. Taken together, these findings suggest that MSCs prevented burn progression by decreasing the susceptibility of cells to apoptosis through an improved balance between antiapoptotic and proapoptotic proteins.

To better understand the cellular events behind the protective effects of MSCs, the contribution of necrosis to cell death in the zone of stasis was evaluated using antibodies against HMGB1. Nuclear-to-cytoplasmic and cytoplasmic-to-extracellular redistribution of HMGB1 was evident in the unburned interspaces of both burn groups, indicating that necrosis is prominent mechanism of cell death during burn injury progression.[29] However, the number of necrotic cells did not differ between both groups. This could be associated with the fact that necrosis in the stasis zone is a passive and unpreventable event that results from the direct effects of the burn.[40]

While inflammation is an integral component of wound healing, a prolonged inflammatory reaction may limit the rate and quality of wound healing.[41] The overabundance of leukocytes, especially neutrophils, is assumed to result in burn wound progression by the overproduction of cytotoxic inflammatory mediators, plugging the microvasculature, and generation of reactive radicals.[42,43] In this study, we documented that MSC transplantation reduced neutrophilic infiltration into the stasis zone, as evidenced by significant reductions in tissue neutrophil count and myeloperoxidase activity. It is thus possible that a reduced inflammatory response may have contributed to the protective effects of MSCs by reducing cytotoxicity, relieving oxidative stress, and preserving vascular patency.

Considering that inflammation is controlled by the balance between proinflammatory and anti-inflammatory factors in a complex cytokine network,[44] we assessed local changes in the expression levels of various inflammatory cytokines. In agreement with previous reports,[45] we found that thermal trauma significantly up-regulated the expression of the proinflammatory cytokines TNF-α, IL-1β, and IL-6 in the stasis zone, and the anti-inflammatory cytokine IL-10 also displayed a corresponding elevation. The activation of such proinflammatory mediators has been implicated as a potential mechanism in many systems as an inductor of apoptosis.[46] On the other hand, MSC transplantation down-regulated the expression of TNF-α, IL-1β, and IL-6 while further elevating IL-10. Taken together, these finding suggest that MSC transplantation ameliorates burn wound progression through an immunomodulatory effect that involves the reduced neutrophilic infiltration, down-regulation

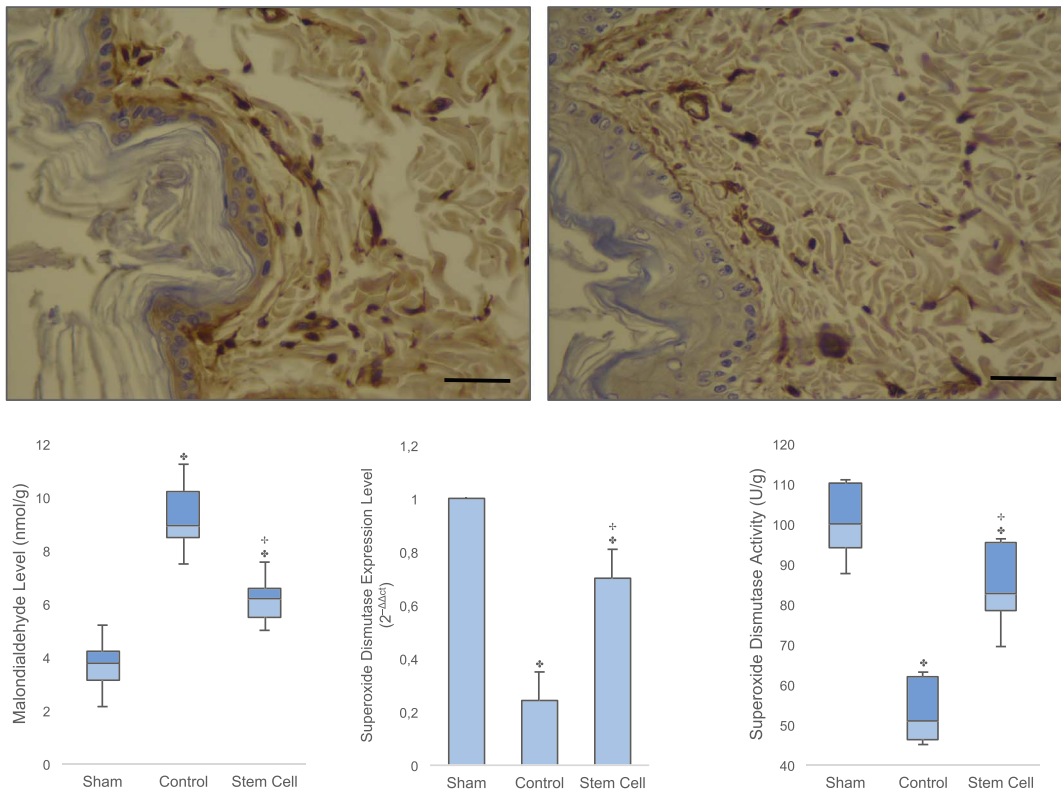

FIGURE 7. Evaluation of oxidative stress in the zone of stasis after the burn using immunohistochemical labeling of malondialdehyde (above). Note higher number of stained cells in the control group (above, left) in comparison with the stem cell group (above, right) (×40 magnification). Scales = 100 μm. Quantitative assessment of malondialdehyde levels (below, left), SOD gene expression levels (below, center), and SOD activity (below, right). The sample size was n = 10 for each group. Data are presented as mean ± SD. ✣$P < 0.001$ versus sham; ✢$P < 0.001$ versus control.

of proinflammatory cytokines, and up-regulation of anti-inflammatory cytokines in the local tissue.

The contribution of oxidative stress on progressive tissue destruction in the stasis zone has been extensively recognized.[47] In the setting of acute burns, the overproduction of reactive oxygen species results in tissue injury by peroxidation of membrane lipids, degradation of proteins, and damage of nucleic acids.[48] In this study, oxidative stress significantly increased after the burn, as shown by increased levels of malondialdehyde. However, MSCs relieved burn-induced oxidative stress in the zone of stasis, which could be associated with the reduced inflammatory response.

While thermal trauma up-regulates free radical production, this type of injury also impairs antioxidant defense mechanisms, rendering burned tissue more susceptible to oxidative injury.[43] In agreement with previous reports,[45,49] we documented significant reductions in the expression and activity of the antioxidant SOD after the burn. This could be associated with the fact that severe levels of oxidative stress may overwhelm antioxidant defense machinery.[50] On the other hand, MSC transplantation significantly reversed burn-induced down-regulation of antioxidant SOD, indicating that MSCs attenuate oxidative stress by the stimulation of endogenous antioxidant enzymes.

Another key factor in the progression of tissue destruction is the impaired blood flow in the stasis zone.[7] In addition to the direct induction of apoptosis and necrosis, impaired blood flow in the deep dermal vascular plexus further compromises the viability of the keratinocytes in the adnexal structures, leading to delayed wound healing.[51] Diminished microcirculation in this partially burned tissue is thought to result from a combination of factors including vasoconstriction, tissue edema, microthrombus formation, neutrophil plugging, and free radical–mediated endothelial injury.[52] In the current study, we showed that MSC-treated interspaces had enhanced vascular density, with scintigraphic evaluation confirming the maintenance and restoration of blood supply. Besides the direct induction neoangiogenesis, the decreased number of CC3a-positive endothelial cells in the stem cell group further supports the idea that MSCs may protect endothelial cells against apoptosis, thereby maintaining their critical functions in the regulation of microvascular blood flow, coagulation, and neutrophil adhesion.

Because we excluded significant engraftment of MSCs into the vasculature, our findings indicate that the obtained proangiogenic effects are mediated mainly by paracrine mechanisms. While the exact underlying mechanisms remain to be determined in further experiments, we evaluated some candidate factors that are known to mediate vasculotropic effects. Higher expression levels for VEGF, PDGF, FGF, and TGF in the stem cell group indicate this mix of factors collectively mediates, at least in part, the vasculotropic properties of MSCs. Characterization of these mediators may lead to the possibility of replacing stem cell–based therapies with soluble factor–based therapies.

The main limitation of the current study is that all assessments were made only at 72 hours after the injury. This timing was chosen in order to investigate the early changes in necrotic and apoptotic cell deaths, inflammatory cell infiltration, oxidative stress, and new vessel formation. However, long-term studies are required to assess long-term results and the reliability of our short-term assessments in predicting them.

CONCLUSIONS

Our data suggest that MSC transplantation into the stasis zone significantly reduced burn wound progression. Although this result is

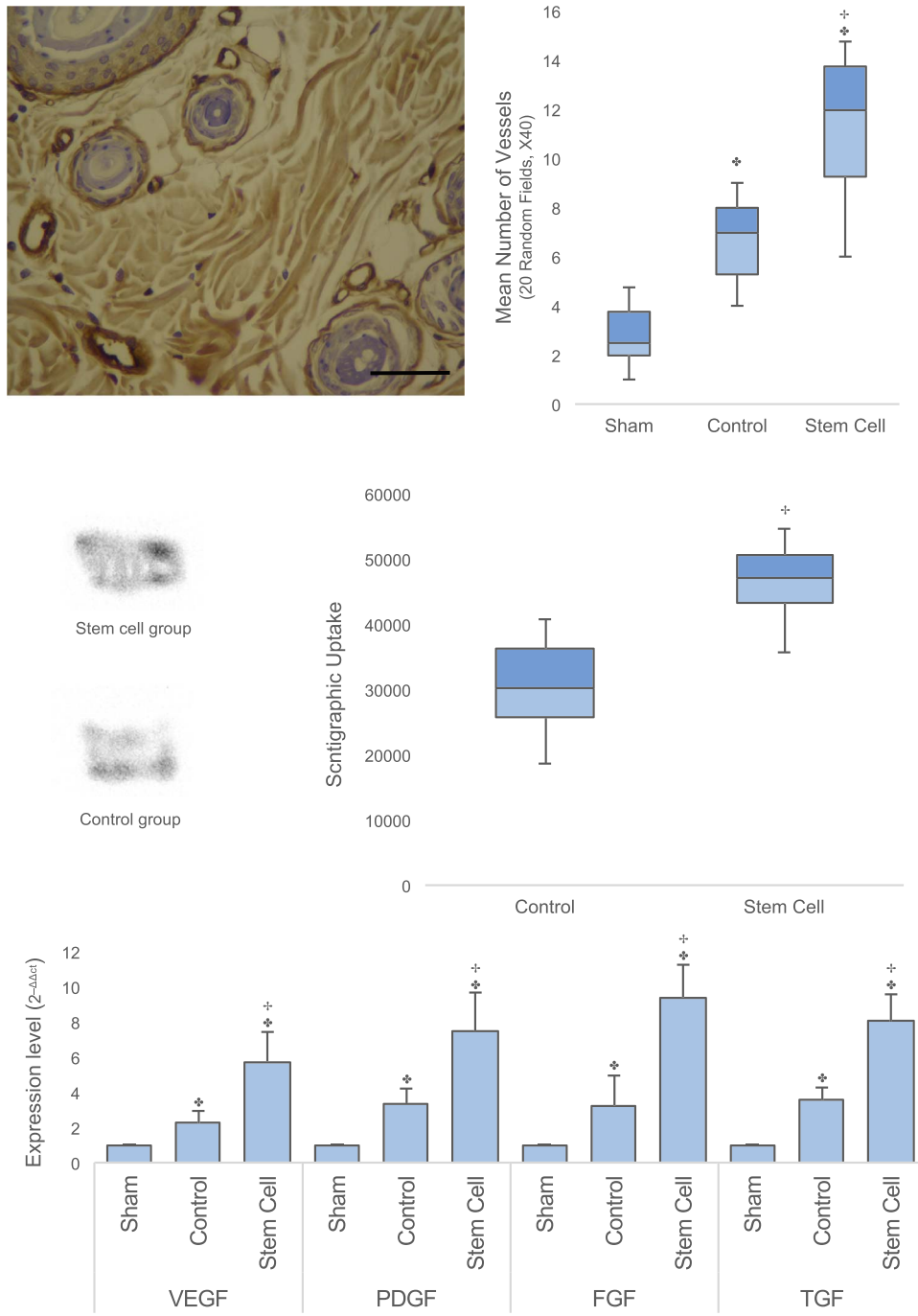

FIGURE 8. Evaluation of microvascular density in the zone of stasis after MSC transplantation using immunohistochemical labeling of CD31 (above, left). Note enhanced microvascular density (×40 magnification). Scale = 100 μm. Quantitative assessment of vascular density (above, right). Representative scintigraphic images of the stem cell and control groups (center, left). Note the obvious borders between the viable and necrotic areas in the image of the stem cell group. Quantitative assessment of scintigraphic uptake (center, right) and angiogenic cytokine expression levels (below). The sample size was n = 10 for each group. Data are presented as mean ± SD. ✣$P < 0.001$ versus sham; ✢$P < 0.001$ versus control.

consistent with the results of previous research, new important findings regarding the underlying mechanisms were obtained. The protective effects of MSCs were mediated by the inhibition of apoptosis through immunomodulatory, antioxidative, and angiogenic actions. However, important questions remain to be answered before clinical translation: what is the better source of MSCs? What is the optimal dose of MSC transplantation? What is the best route of MSC administration? Do MSCs integrate into the tissue to replace damaged cells during longer follow-up periods?

REFERENCES

1. Jackson DM. The diagnosis of the depth of burning. *Br J Surg*. 1953;40:588–596.
2. Kao CC, Garner WL. Acute burns. *Plast Reconstr Surg*. 2000;101:2482–2493.
3. Johnson RM, Richard R. Partial-thickness burns: identification and management. *Adv Skin Wound Care*. 2003;16:178–187; quiz 88–9.
4. Gravante G, Filingeri V, Delogu D, et al. Apoptotic cell death in deep partial thickness burns by coexpression analysis of TUNEL and Fas. *Surgery*. 2006;139: 854–855.
5. Gravante G, Palmieri MB, Esposito G, et al. Apoptotic death in deep partial thickness burns vs. normal skin of burned patients. *J Surg Res*. 2007;141:141–145.
6. Contassot E, Gaide O, French LE. Death receptors and apoptosis. *Dermatol Clin*. 2007;25:487–501, vii.
7. Shupp JW, Nasabzadeh TJ, Rosenthal DS, et al. A review of the local pathophysiologic bases of burn wound progression. *J Burn Care Res*. 2010;31:849–873.
8. Sharma RR, Pollock K, Hubel A, et al. Mesenchymal stem or stromal cells: a review of clinical applications and manufacturing practices. *Transfusion*. 2014;54: 1418–1437.
9. Riccobono D, Agay D, Scherthan H, et al. Application of adipocyte-derived stem cells in treatment of cutaneous radiation syndrome. *Health Phys*. 2012;103: 120–126.
10. Xue L, Xu YB, Xie JL, et al. Effects of human bone marrow mesenchymal stem cells on burn injury healing in a mouse model. *Int J Clin Exp Pathol*. 2013;6: 1327–1336.
11. Ha XQ, Lu TD, Hui L, et al. Effects of mesenchymal stem cells transfected with human hepatocyte growth factor gene on healing of burn wounds. *Chin J Traumatol*. 2010;13:349–355.
12. Bey E, Prat M, Duhamel P, et al. Emerging therapy for improving wound repair of severe radiation burns using local bone marrow–derived stem cell administrations. *Wound Repair Regen*. 2010;18:50–58.
13. Rasulov MF, Vasilchenkov AV, Onishchenko NA, et al. First experience of the use bone marrow mesenchymal stem cells for the treatment of a patient with deep skin burns. *Bull Exp Biol Med*. 2005;139:141–144.
14. Liu L, Yu Y, Hou Y, et al. Human umbilical cord mesenchymal stem cells transplantation promotes cutaneous wound healing of severe burned rats. *PLoS One*. 2014;9:e88348.
15. Shumakov VI, Onishchenko NA, Rasulov MF, et al. Mesenchymal bone marrow stem cells more effectively stimulate regeneration of deep burn wounds than embryonic fibroblasts. *Bull Exp Biol Med*. 2003;136:192–195.
16. Agay D, Scherthan H, Forcheron F, et al. Multipotent mesenchymal stem cell grafting to treat cutaneous radiation syndrome: development of a new minipig model. *Exp Hematol*. 2010;38:945–956.
17. Mansilla E, Spretz R, Larsen G, et al. Outstanding survival and regeneration process by the use of intelligent acellular dermal matrices and mesenchymal stem cells in a burn pig model. *Transplant Proc*. 2010;42:4275–4278.
18. Yang Y, Zhang W, Li Y, et al. Scalded skin of rat treated by using fibrin glue combined with allogeneic bone marrow mesenchymal stem cells. *Ann Dermatol*. 2014;26:289–295.
19. Yan G, Sun H, Wang F, et al. Topical application of hPDGF-A–modified porcine BMSC and keratinocytes loaded on acellular HAM promotes the healing of combined radiation-wound skin injury in minipigs. *Int J Radiat Biol*. 2011;87: 591–600.
20. Hao L, Wang J, Zou Z, et al. Transplantation of BMSCs expressing hPDGF-A/hBD2 promotes wound healing in rats with combined radiation-wound injury. *Gene Ther*. 2009;16:34–42.
21. Xia Z, Zhang C, Zeng Y, et al. Transplantation of BMSCs expressing hVEGF165/hBD3 promotes wound healing in rats with combined radiation-wound injury. *Int Wound J*. 2014;11:293–303.
22. Loder S, Peterson JR, Agarwal S, et al. Wound healing after thermal injury is improved by fat and adipose-derived stem cell isografts. *J Burn Care Res*. 2015;36: 70–76.
23. Öksüz S, Ulkur E, Oncul O, et al. The effect of subcutaneous mesenchymal stem cell injection on statis zone and apoptosis in an experimental burn model. *Plast Reconstr Surg*. 2013;131:463–471.
24. Singer DD, Singer AJ, Gordon C, et al. The effects of rat mesenchymal stem cells on injury progression in a rat model. *Acad Emerg Med*. 2013;20:398–402.
25. Calio ML, Marinho DS, Ko GM, et al. Transplantation of bone marrow mesenchymal stem cells decreases oxidative stress, apoptosis, and hippocampal damage in brain of a spontaneous stroke model. *Free Radic Biol Med*. 2014;70:141–154.
26. Regas FC, Ehrlich HP. Elucidating the vascular response to burns with a new rat model. *J Trauma*. 1992;32:557–563.
27. Isik S, Sahin U, Ilgan S, et al. Saving the zone of stasis in burns with recombinant tissue-type plasminogen activator (r-tPA): an experimental study in rats. *Burns*. 1998;24:217–223.
28. Iseri SO, Dusunceli F, Erzik C, et al. Oxytocin or social housing alleviates local burn injury in rats. *J Surg Res*. 2010;162:122–131.
29. Singer AJ, McClain SA, Taira BR, et al. Apoptosis and necrosis in the ischemic zone adjacent to third degree burns. *Acad Emerg Med*. 2008;15:549–554.
30. Mateos R, Lecumberri E, Ramos S, et al. Determination of malondialdehyde (MDA) by high-performance liquid chromatography in serum and liver as a biomarker for oxidative stress. Application to a rat model for hypercholesterolemia and evaluation of the effect of diets rich in phenolic antioxidants from fruits. *J Chromatogr B Analyt Technol Biomed Life Sci*. 2005;827:76–82.
31. Fitzgerald SP CJ, Lamont JV, eds. The establishment of reference ranges for selenium. The selenoenzyme glutathione peroxidase and the metalloenzyme superoxide dismutase in blood fraction. The Fifth International Symposium on Selenium Biology and Medicine. Tennessee; 1992.
32. Hillegass LM, Griswold DE, Brickson B, et al. Assessment of myeloperoxidase activity in whole rat kidney. *J Pharmacol Methods*. 1990;24:285–295.
33. Reddy GK, Enwemeka CS. A simplified method for the analysis of hydroxyproline in biological tissues. *Clin Biochem*. 1996;29:225–229.
34. Carvalho AC, Sharpe J, Rosenstock TR, et al. Bax affects intracellular Ca^{2+} stores and induces Ca^{2+} wave propagation. *Cell Death Differ*. 2004;11:1265–1276.
35. Floros KV, Thomadaki H, Katsaros N, et al. mRNA expression analysis of a variety of apoptosis-related genes, including the novel gene of the BCL2-family, BCL2L12, in HL-60 leukemia cells after treatment with carboplatin and doxorubicin. *Biol Chem*. 2004;385:1099–1103.
36. McGonigle P, Ruggeri B. Animal models of human disease: challenges in enabling translation. *Biochem Pharmacol*. 2014;87:162–171.
37. Li X, Liu L, Yang J, et al. Exosome derived from human umbilical cord mesenchymal stem cell mediates MiR-181c attenuating burn-induced excessive inflammation. *EBioMedicine*. 2016;8:72–82.
38. Zhao B, Zhang Y, Han S, et al. Exosomes derived from human amniotic epithelial cells accelerate wound healing and inhibit scar formation. *J Mol Histol*. 2017;48: 121–132.
39. Na YK, Ban JJ, Lee M, et al. Wound healing potential of adipose tissue stem cell extract. *Biochem Biophys Res Commun*. 2017;485:30–34.
40. Fink SL, Cookson BT. Apoptosis, pyroptosis, and necrosis: mechanistic description of dead and dying eukaryotic cells. *Infect Immun*. 2005;73:1907–1916.
41. Suber F, Carroll MC, Moore FD Jr. Innate response to self-antigen significantly exacerbates burn wound depth. *Proc Natl Acad Sci U S A*. 2007;104:3973–3977.
42. Bucky LP, Vedder NB, Hong HZ, et al. Reduction of burn injury by inhibiting CD18-mediated leukocyte adherence in rabbits. *Plast Reconstr Surg*. 1994;93: 1473–1480.
43. Parihar A, Parihar MS, Milner S, et al. Oxidative stress and anti-oxidative mobilization in burn injury. *Burns*. 2008;34:6–17.
44. Zhang JM, An J. Cytokines, inflammation, and pain. *Int Anesthesiol Clin*. 2007; 45:27–37.
45. Guo SX, Jin YY, Fang Q, et al. Beneficial effects of hydrogen-rich saline on early burn-wound progression in rats. *PLoS One*. 2015;10:e0124897.
46. Baker SJ, Reddy EP. Modulation of life and death by the TNF receptor superfamily. *Oncogene*. 1998;17:3261–3270.
47. Latha B, Babu M. The involvement of free radicals in burn injury: a review. *Burns*. 2001;27:309–317.
48. Horton JW. Free radicals and lipid peroxidation mediated injury in burn trauma: the role of antioxidant therapy. *Toxicology*. 2003;189:75–88.
49. Emamgholipour S, Hossein-Nezhad A, Ansari M. Can melatonin act as an antioxidant in hydrogen peroxide-induced oxidative stress model in human peripheral blood mononuclear cells? *Biochem Res Int*. 2016;2016:5857940.
50. Ercal N, Gurer-Orhan H, Aykin-Burns N. Toxic metals and oxidative stress part I: mechanisms involved in metal-induced oxidative damage. *Curr Top Med Chem*. 2001;1:529–539.
51. Papp A, Romppanen E, Lahtinen T, et al. Red blood cell and tissue water content in experimental thermal injury. *Burns*. 2005;31:1003–1006.
52. Baskaran H, Toner M, Yarmush ML, et al. Poloxamer-188 improves capillary blood flow and tissue viability in a cutaneous burn wound. *J Surg Res*. 2001; 101:56–61.